Development 134, 3021-3029 (2007) doi:10.1242/dev.02874

Fgf8 induces pillar cell fate and regulates cellular patterning in the mammalian cochlea

Bonnie E. Jacques[1,2], Mireille E. Montcouquiol[1,*], Erynn M. Layman[1], Mark Lewandoski[3] and Matthew W. Kelley[1,†]

The mammalian auditory sensory epithelium (the organ of Corti) contains a number of unique cell types that are arranged in ordered rows. Two of these cell types, inner and outer pillar cells (PCs), are arranged in adjacent rows that form a boundary between a single row of inner hair cells and three rows of outer hair cells (OHCs). PCs are required for auditory function, as mice lacking PCs owing to a mutation in *Fgfr3* are deaf. Here, using in vitro and in vivo techniques, we demonstrate that an Fgf8 signal arising from the inner hair cells is the key component in an inductive pathway that regulates the number, position and rate of development of PCs. Deletion of *Fgf8* or inhibition of binding between Fgf8 and Fgfr3 leads to defects in PC development, whereas overexpression of Fgf8 or exogenous Fgfr3 activation induces ectopic PC formation and inhibits OHC development. These results suggest that Fgf8-Fgfr3 interactions regulate cellular patterning within the organ of Corti through the induction of one cell fate (PC) and simultaneous inhibition of an alternate fate (OHC) in separate progenitor cells. Some of the effects of both inhibition and overactivation of the Fgf8-Fgfr3 signaling pathway are reversible, suggesting that PC differentiation is dependent upon constant activation of Fgfr3 by Fgf8. These results suggest that PCs might exist in a transient state of differentiation that makes them potential targets for regenerative therapies.

KEY WORDS: Organ of Corti, Hair cell, Fgfr3, Mouse

INTRODUCTION

The sensory epithelium of the mammalian cochlea, the organ of Corti (OC), comprises at least six distinct cell types arranged into precise rows that extend along the entire length of the cochlear spiral. The OC contains four rows of hair cells (Fig. 1A): three rows of outer hair cells (OHCs) supported by underlying Deiter's cells (DCs) and flanked on the lateral edge by a several rows of Hensen's cells (HeCs), and one row of inner hair cells (IHCs) with underlying phallangeal cells. Separating the two types of hair cells are parallel rows of non-sensory pillar cells (PCs) (Fig. 1B). When mature, PCs form the boundaries of a triangular fluid-filled space referred to as the tunnel of Corti (Fig. 1C) (Raphael and Altschuler, 2003). The tunnel of Corti and the PCs that form this structure are unique to the mammalian auditory system and are found in no other vertebrate class. Defects in PC development result in significant hearing impairment (Colvin et al., 1996).

Despite their crucial role in cochlear function, the factors that regulate PC formation are poorly understood. Previous work has demonstrated that ongoing activation of one of the fibroblast growth factor receptors, Fgfr3, is required for PC development (Colvin et al., 1996; Mueller et al., 2002). Ectopic activation of Fgfr3 in vitro by treatment with Fgf2 induces an overproduction of PCs, suggesting that the relative level of ligand available for Fgfr3 activation plays a key role in regulating PC number and position within the OC (Mueller et al., 2002). Fgfr3 is one of four related receptors that bind to members of the fibroblast growth factor family. All Fgf receptors are transmembrane proteins that contain a tyrosine kinase (TK) domain in their intracellular region. Fgfr activation is mediated through binding of one of at least 23 known Fgfs and a sulfated glycosaminoglycan such as heparin sulfate. Binding of Fgf ligand and heparin leads to receptor dimerization, cross-activation of the TK domains and downstream signaling through the MAP kinase signaling pathway (Mohammadi et al., 2005).

Within the developing cochlea, Fgfr3 is initially expressed at ~E16 in a broad pool of progenitor cells located directly adjacent to developing IHCs (Mueller et al., 2002; Peters et al., 1993), the first cells to differentiate within the epithelium (Sobin and Anniko, 1984). Based on the spatiotemporal pattern of expression, it seems likely that Fgfr3 is expressed in progenitors that will ultimately develop as PCs and OHCs, as well as HeCs and DCs. As development proceeds, Fgfr3 is downregulated in progenitors that develop as OHCs, HeCs and DCs, but is maintained in PCs (Mueller et al., 2002; Pirvola et al., 1995). RNA expression analysis using quantitative PCR has suggested that the *Fgfr3c* splice variant is the predominant isoform expressed in the cochlea (Pickles, 2001). In addition, ligand-binding assays indicate that the 'c' isoform of Fgfr3 binds to the Fgf8b isoform with high affinity (MacArthur et al., 1995; Olsen et al., 2006; Ornitz et al., 1996). The Fgf8b ligand has been shown to have important regulatory roles during pattern formation, differentiation and cell growth throughout the developing embryo and nervous system (Olsen et al., 2006). Quantitative RT-PCR analysis has indicated that it is expressed in the embryonic cochlear sensory epithelium (Pickles, 2001). Here, we demonstrate that *Fgf8* is expressed in a pattern that is consistent with an inductive role in PC development and that changes in the levels of Fgf8, or in Fgfr3 activation, lead to corresponding changes in the number and differentiation of PCs.

[1]Section on Developmental Neuroscience, Porter Neuroscience Research Center, 35 Convent Dr, Room 2A-100, National Institute on Deafness and Other Communication Disorders, National Institutes of Health, Bethesda, MD 20892, USA. [2]University of Maryland College Park, Department of Biology, College Park, MD, USA. [3]Genetics of Vertebrate Development Section, Cancer and Developmental Biology Laboratory, National Cancer Institute, Frederick, MD, USA.

*Present address: Equipe AVENIR 2 'Neurosciences Dévelopementales' IFR8, INSERM, Institut F. Magendie des Neurosciences, 33077 Bordeaux Cedex, France
†Author for correspondence (e-mail: kelleymt@nidcd.nih.gov)

Accepted 29 May 2007

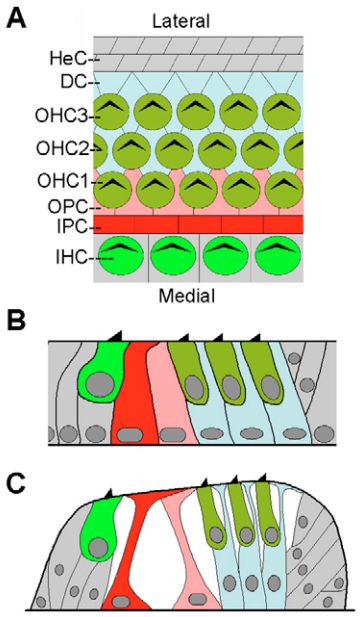

Fig. 1. Anatomy of the mouse organ of Corti. (**A**) Diagram of the lumenal surface of the organ of Corti (OC) at P0. A row of alternating inner hair cells (light green) and phalangeal cells (gray) are bordered by one row of inner PCs (red) and one row of outer pillar cells (PCs, pink). Outer PCs project between first-row outer hair cells (OHCs, olive green). Second and third row OHCs are separated by Deiter's cells (DC, blue). Hensen's cells (HeC, gray) form the lateral edge of the OC. (**B**,**C**) Cross-sections of the OC at (B) P0 and (C) adult.

MATERIALS AND METHODS

In situ hybridization

In situ hybridization (ISH) was performed as described previously (Wu and Oh, 1996) for *Fgf8* and *Fgfr3* on 12 μm frozen sections or whole organs from cochleae isolated at E15, E16 and P0. A probe specific to exons 2 and 3 of *Fgf8* (the region excised by Cre in the $Fgf8^{\Delta 2,3n/flox}$; $Foxg1^{cre/+}$ mutants) was also used on E16-18 cochleae from $Fgf8^{\Delta 2,3n/flox}$; $Foxg1^{cre/+}$ mutants and their wild-type littermates to demonstrate excision of the targeted region.

Generation of $Fgf8^{\Delta 2,3n/flox}$; $Foxg1^{cre/+}$ mutants and analysis of pillar cell defects

Animals with a targeted deletion of *Fgf8* in the forebrain, retina and inner ear were generated by crossing $Fgf8^{flox/flox}$ females with $Fgf8^{\Delta 2,3n/+}$; $Foxg1^{cre/+}$ males. Mice carrying these alleles have been described previously (Meyers et al., 1998; Hebert and McConnell, 2000). Mutant progeny of the genotype $Fgf8^{\Delta 2,3n/flox}$; $Foxg1^{cre/+}$ were visually identified based on obvious defects in the development of the forebrain (Storm et al., 2003). Siblings were of the genotypes $Fgf8^{+/flox}$; $Foxg1^{cre/+}$, $Fgf8^{+/flox}$; $Foxg1^{+/+}$ or $Fgf8^{\Delta 2,3n/flox}$; $Foxg1^{+/+}$ and served as normal littermate controls. Cochleae were dissected from mutants and littermate controls at E15.5, E16 and E19, and fixed in either 4% paraformaldehyde (PFA) or 3% glutaraldehyde/2% PFA overnight. Following fixation, the cochleae were dissected and the OC were exposed and labeled with cell type-specific antibodies: anti-myosin VI (Proteus Biosciences) 1:1000; anti-$p75^{ntr}$ (Chemicon) 1:1000; anti-β-actin (Sigma) 1:200. Secondary antibodies were conjugated to one of the following: Alexa 350, Alexa 488, Alexa 546 or Alexa 633 (Molecular Probes). In addition, filamentous actin was labeled using phalloidin at 1:200 conjugated to either Alexa 488 or Alexa 633 (Molecular Probes). Specimens were then flat-mounted and the total length of the cochlear duct was measured. The cochlea was then divided into four equal sections, each representing a quarter of the total length of the cochlear duct, and the distances between the inner hair cells and first row of outer hair cells (ITO distances) were determined in each region (n=5 animals; greater than 50 cells counted per region). All animal care and procedures were approved by the Animal Care and Use Committee at NIH and complied with the NIH guidelines for the care and use of animals.

Measurement of ITO distance

The inner-to-outer (ITO) distance is defined as the distance between the lateral edge of the IHC and the medial edge of the first row OHC. This is the distance encompassed by the inner pillar head. Digital images of the OC were captured for each sample using a Zeiss 510 LSM confocal laser-scanning microscope. Measurements of ITO distances were taken at three specific points along the length of the cochlear duct of each sample, roughly at 25%, 50% and 75% of the distance from the most basal region and moving towards the apex. A minimum of 15 ITO measurements were made at each of the three locations. Cell counts were also taken of each cell type in the measured quadrants.

Histological sections

Temporal bones from control and $Fgf8^{\Delta 2,3n/+}$; $Foxg1^{cre/+}$ littermates were fixed in 3% glutaraldehyde/2% paraformaldehyde, tissue was dehydrated in ethanol and then embedded in Immunobed (Polysciences). Cochleae were oriented to generate mid-modiolar sections, cut at 5 μm and stained with thionin.

Explant cultures

Explant cultures of embryonic cochleae were established as described previously (Montcouquiol and Kelley, 2003) and maintained for 6 DIV. E13.5 explants were incubated for 24 hours before exposure to growth factors or antibodies that were diluted in culture medium to the stated final concentrations along with 0.1% DMSO and 1 μg/μl heparin. Anti-Fgf8b, 75-150 μg/ml; anti-Fgf5, 75-150 μg/ml; Fgf17, 300 ng/ml (all from R&D systems). Antibodies and proteins were used at 100 times the ND_{50} and ED_{50}, to ensure penetration through the reticular lamina, a strong ionic barrier that exists at the lumenal surface of the OC.

Electroporation

Full-length cDNA for murine *Fgf8b* was kindly provided by Elizabeth Grove, University of Chicago (Fukuchi-Shimogori and Grove, 2001). *Fgf8b* was excised from its original vector using *Bam*HI and then directly ligated into the pAM/CAG-IRES_EGFP vector at the *Bam*HI site. Orientation was determined by sequencing. Empty pAM/CAG-IRES_EGFP vector and pAM/CAG-IRES_EGFP containing full-length *Fgf8b* in the reverse orientation were used as controls. Electroporation of cochlear explants was carried out as previously described (Jones et al., 2006); n>30 for each vector type.

Luminosity measurements

Images of electroporated explants were obtained using a Zeiss LSM510 confocal microscope. All samples were obtained during the same session using the same laser power and detection settings. To quantify the effects of overexpression of *Fgf8*, a rectangle (225 μm×110 μm) was oriented such that the short dimension of the rectangle was parallel with the line of PCs in the region being measured. The rectangle was positioned so that its strial edge aligned with third row OHCs. Thus, the rectangle included a 110 μm stretch of the OC with the adjacent region of the greater epithelial ridge containing transfected cells. Control and experimental regions were obtained and then thresholded for both green and red pixels. The total number of pixels of each color was then determined as a percentage of the total of number of pixels within the entire rectangle.

RESULTS

Expression of *Fgf8* and *Fgfr3* in the organ of Corti

PCs develop on the medial edge of an *Fgfr3*-expression domain located directly adjacent to the IHCs. Given the crucial role of Fgfr3 in PC formation (Mueller et al., 2002; Pirvola et al., 1995), it seemed likely that hair cells located adjacent to developing PCs might act as a source of ligand for Fgfr3. Furthermore, Fgf8, a high affinity ligand for Fgfr3, has been reported to be expressed by the IHCs of the adult cochlea (Pirvola et al., 2002; Shim et al., 2005). To

determine whether Fgf8 could play a role in PC development, the expression pattern for *Fgf8* in the embryonic cochlea was compared with that of *Fgfr3* by ISH. Cochlear development proceeds in a spatially conserved pattern in which cells in the basal region mature prior to those in the apical region, allowing one to visualize multiple developmental stages within the same ear (Sobin and Anniko, 1984). No expression of *Fgf8* was observed between E13 and E15 (data not shown) or at E16 in the less mature apex (Fig. 2A). However, *Fgf8* expression was observed in a single cell in the more mature basal region at E16 (Fig. 2B). *Fgfr3* expression was also first observed in the basal region of the cochlea at E16 in a group of cells that correlates with developing PCs, OHCs, HeCs and DCs (Fig. 2D). Weak expression of *Fgfr3* was observed in the apex of the same E16 cochlea (Fig. 2C), suggesting that its onset might slightly precede that of *Fgf8*. By P0, *Fgf8* expression was clearly present in the single IHC (Fig. 2E,G), whereas expression of *Fgfr3* had largely become restricted to the developing PCs (Fig. 2F). Some expression of *Fgfr3* persisted in the developing DC and HeC region (Fig. 2F); however, based on immunolocalization, this expression appears to be downregulated as development continues (Mueller et al., 2002). These expression patterns demonstrate that the timing of the onset of *Fgf8* expression correlates strongly with the onset of *Fgfr3* expression and subsequent differentiation of PCs.

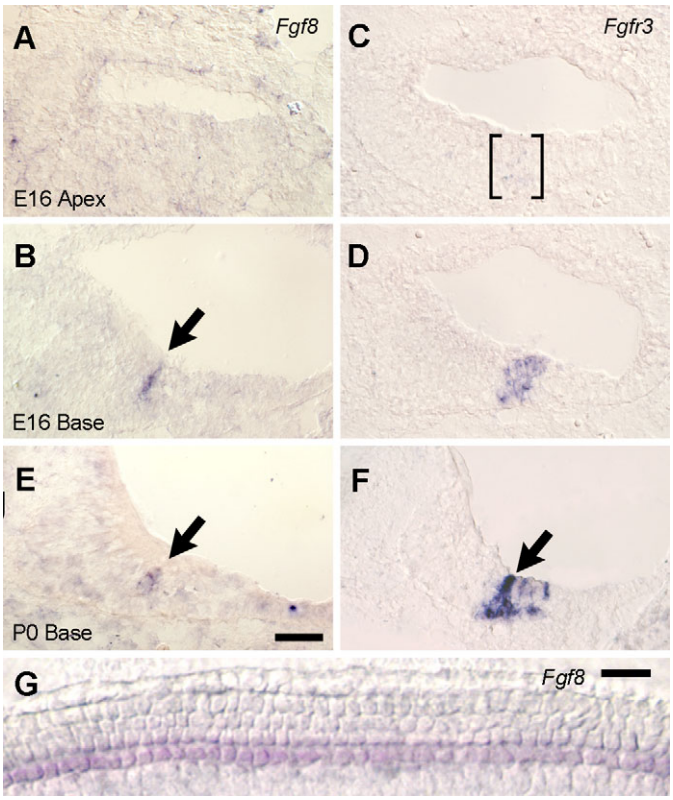

Fig. 2. *Fgf8* and *Fgfr3* are expressed in the developing organ of Corti. In situ hybridizations for *Fgf8* and *Fgfr3* were performed on E16 (**A-D**) and P0 (**E-G**) mice. *Fgf8* is not detected at E16 in the apical region (A), but is seen in developing IHCs at the base (B, arrow). (C) At E16, *Fgfr3* is faintly detected in a group of cells near the apex (indicated by brackets) and shows more robust expression within a similar region at the base (D). (E) Expression of *Fgf8* at P0 is in the IHC (arrow), whereas *Fgfr3* (F) is restricted to PCs (arrow) and DCs. (G) Whole-mount of the lumenal surface at P0 illustrating expression of *Fgf8* in all IHCs. Scale bars: 30 μm in A-F; 20 μm in G.

Deletion of *Fgf8* in vivo results in defects in pillar cell development

To determine whether Fgf8 is required for PC development, a tissue-specific deletion of *Fgf8* was generated using a Cre-loxP strategy. Briefly, a floxed version of *Fgf8* (*Fgf8*^{flox}) (Meyers et al., 1998) and the *Foxg1*^{cre} line (Hebert and McConnell, 2000) were used to delete *Fgf8* in a subset of tissues. It has been demonstrated that Cre-mediated excision of the second and third exons of the *Fgf8*^{flox} allele results in complete inactivation (Meyers et al., 1998). The *Foxg1* promoter induces expression of *Cre* in a relatively small number of tissues, including the developing otocyst, beginning at E8.5. By E9, the expression of *Cre* is strong in virtually all cells within the otocyst (Hebert and McConnell, 2000), well before the normal onset of *Fgf8* expression.

Embryos that were *Fgf8*$^{\Delta 2,3n/flox}$; *Foxg1*$^{cre/+}$ (see Materials and methods for specific genetic cross) die at birth as a result of defects in the development of the forebrain (Storm et al., 2003); however, overall development of the inner ear and cochlea appeared normal. To examine the effects of inactivation of *Fgf8* on PC development, cochleae were obtained from mutants at E15 and E18.5. Consistent with the timing of the onset of *Fgf8*, there were no obvious differences in cellular patterning or in the expression of p75^{ntr} (a marker that is co-expressed with Fgfr3 during cochlear development; also known as Ngfr – Mouse Genome Informatics) (Mueller et al., 2002) between mutants and controls at E15 (data not shown). Although development of IHCs and OHCs appeared normal at E18.5 (Fig. 3A,B), there was a marked decrease in the size and number of PCs as well as a decrease in the overall levels of expression of p75^{ntr}, both in the PCs and HeCs (Fig. 3C,D). The effects of deletion of *Fgf8* were quantified by determining the distance between IHCs and OHCs, referred to as the ITO distance (Mueller et al., 2002), at different positions along the basal-to-apical axis of the OC. The developing pillar heads expand as the cells differentiate and thus larger ITO distances are reflective of more advanced PC development (Mueller et al., 2002). Deletion of *Fgf8* resulted in a significant decrease in ITO distances along the length of the cochlea (Fig. 3G), similar to that seen in *Fgfr3*-knockout mice (B.E.J., C. Puligilla and M.W.K., unpublished).

Rather than a complete absence of p75^{ntr}-positive PCs, as seen when Fgfr3 is pharmacologically inhibited (Colvin et al., 1996; Mueller et al., 2002), some p75^{ntr}-positive cells were clearly present in the PC space in *Fgf8*$^{\Delta 2,3n/flox}$; *Foxg1*$^{cre/+}$ mutants (Fig. 3D). Therefore, semi-thin plastic cross-sections of the cochlea from *Fgf8*$^{\Delta 2,3n/flox}$; *Foxg1*$^{cre/+}$ mice were examined at E15 (n=4) and E18.5 (n=5). As expected based on the timing of onset of *Fgf8* expression, overall structure of the epithelium and putative developing PCs appeared normal in cross-sections from E15 (data not shown). By contrast, at E18.5, two cells were present in the region of the epithelium between the IHCs and OHCs (Fig. 3E,F), but these cells had either weak lumenal projections or no projections at all. In some sections, the IHCs and OHCs appeared to be in direct contact with eachother (Fig. 3F, magnified in inset with a red line to show the IHC boundary and a green line to show the OHC boundary). PCs with weak or no lumenal projections were observed along the entire length of the cochlea with no region-specific variations. To ensure that Cre-mediated excision of *Fgf8* exons 2 and 3 was complete in these mutants, ISH was performed on *Fgf8*$^{\Delta 2,3n/flox}$; *Foxg1*$^{cre/+}$ mutants and their control littermates (n>3 for each genotype analyzed) at E16-18 using a probe generated from exons 2 and 3 of the *Fgf8* gene. Control and mutant cochleae were processed together and the colorization step was deliberately extended to ensure detection of any residual *Fgf8*. A single row of *Fgf8*-positive IHCs

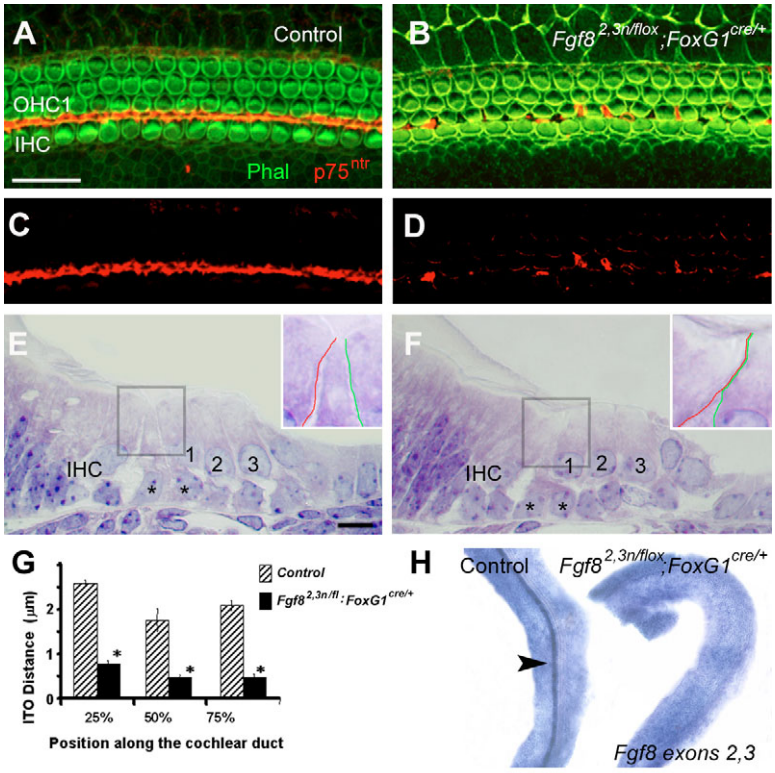

Fig. 3. Targeted deletion of *Fgf8* leads to a disruption in pillar cell development. (**A**) Lumenal suface of the OC from a littermate control at E18.5. Hair cell stereocilia and cell boundaries labeled with phalloidin (Phal, green) and PCs labeled with anti-p75^{ntr} (red). The row of IHCs and first row of OHCs (OHC1) are indicated. (**B**) Lumenal surface from an *Fgf8*$^{\Delta 2,3n/flox}$; *Foxg1*$^{cre/+}$ mouse. Note the disrupted growth of the PCs and close approximation of the IHCs to OHCs. (**C**,**D**) Red channels from A and B, respectively, illustrating PC morphology. (D) PCs are missing or underdeveloped in *Fgf8*$^{\Delta 2,3n/flox}$; *Foxg1*$^{cre/+}$ mice. (**E**) Cross-section through a control OC at E18.5 showing two PCs (asterisks) extending a lumenal projection between the IHC and first row OHC (numbered). Magnification of the boxed region (inset) illustrates the morphology of the projection, with a red line to indicate the lateral boundary of the IHC and a green line to indicate the medial boundary of the first row OHC. (**F**) Cross-section through an *Fgf8*$^{\Delta 2,3n/flox}$; *Foxg1*$^{cre/+}$ OC illustrating a stunted lumenal PC projection (magnified in inset). (**G**) Average ITO distances (see text for details), as a measure of the degree of PC development, in control and *Fgf8*$^{\Delta 2,3n/flox}$; *Foxg1*$^{cre/+}$ cochleae. Error bars indicate s.e.m. *, $P<0.001$. (**H**) In situ hybridization using a probe specific to the deleted region of *Fgf8* in control and *Fgf8*$^{\Delta 2,3n/flox}$; *Foxg1*$^{cre/+}$ cochleae. Arrowhead points to the row of labeled IHCs in the control; no such labeling is apparent in the *Fgf8*$^{\Delta 2,3n/flox}$; *Foxg1*$^{cre/+}$ cochlea. Both cochleae have been intentionally over-reacted to ensure complete detection of *Fgf8* expression. Scale bars: 20 μm in A-D; 10 μm in E,F.

was clearly present in control cochleae; however, no expression of *Fgf8* was observed in the mutant cochleae (Fig. 3H). These results indicate a complete deletion of *Fgf8* in *Fgf8*$^{\Delta 2,3n/flox}$; *Foxg1*$^{cre/+}$ mutants.

In vitro treatment with an anti-Fgf8 antibody results in complete inhibition of pillar cell development

The presence of some p75^{ntr}-positive inner PCs in *Fgf8*$^{\Delta 2,3n/flox}$; *Foxg1*$^{cre/+}$ mutants, compared with the complete absence of these cells in cochlear explants in which Fgfr3 activation has been inhibited (Mueller et al., 2002), suggests possible residual Fgfr3 activity in *Fgf8*$^{\Delta 2,3n/flox}$; *Foxg1*$^{cre/+}$ mutants. This could be the result of functional compensation within the Fgf8-deficient mutant cochleae, whereby another endogenously expressed Fgf may bind to and activate Fgfr3 when no Fgf8 ligand is present. Therefore, we sought to inhibit Fgf8 signaling at the protein level using an Fgf8-function-blocking antibody on cochlear explant cultures. As a control, similar explants were exposed to an antibody that specifically blocks the function of Fgf5, a ligand not reported to be endogenously expressed within the OC. Explants were established on E13, exposed to anti-Fgf8 beginning after 24-36 hours, maintained for 4 to 6 days in vitro (DIV), then fixed and stained to examine PC development. Exposure to anti-Fgf8 resulted in a complete loss of p75^{ntr} labeling, a lack of obvious pillar heads (Fig. 4C) and ITO distances approaching zero (Fig. 4D), indicating a complete inhibition of PC development. This effect phenocopies that observed in explants exposed to the Fgfr antagonist SU5402 (Mueller et al., 2002). By contrast, exposure to anti-Fgf5 had no apparent effect on PC development (Fig. 4B,D). If the addition of anti-Fgf8 was delayed until the equivalent of E17, reductions in p75^{ntr} staining and ITO distance were observed, but their magnitude was decreased compared with those observed upon exposure to anti-Fgf8 for 6 DIV (data not shown). Similarly, a 72-hour transient exposure to anti-Fgf8 beginning at E14.5 resulted in a decrease in ITO distances that was consistent with a delay in the onset of PC differentiation (data not shown). Based on these results, there appears to be an ongoing requirement for Fgf8 throughout the 5-day period of embryonic PC development. The complete inhibition of pillar head formation in these explants, in contrast to the small residual development in *Fgf8*$^{\Delta 2,3n/flox}$; *Foxg1*$^{cre/+}$ mutants, suggests that either *Fgf8* was not completely deleted in the *Fgf8*$^{\Delta 2,3n/flox}$; *Foxg1*$^{cre/+}$ mutants, or that the anti-Fgf8 antibody recognizes and inhibits other Fgfs within the epithelium that also activate Fgfr3. The first explanation seems less likely, considering that ISH indicated no expression of *Fgf8* mRNA at E16.5. By contrast, *Fgf10* is expressed in the developing inner sulcus (Pauley et al., 2003), and preliminary results indicate that *Fgf17* is also expressed in the cochlea (B.E.J., K. L. Mueller and M.W.K., unpublished).

Ectopic Fgf8 expression results in overexpression of pillar cell markers

It has been shown that addition of exogenous Fgf2 results in the formation of additional rows of PCs (Mueller et al., 2002), suggesting that the amount of Fgf within the epithelium could be a limiting factor in PC formation. Therefore, the effects of increased Fgf8 within the cochlea were determined by transfecting cochlear explants with an *Fgf8* expression vector containing *EGFP* as an independent transcript to identify transfected cells (Fukuchi-Shimogori and Grove, 2003; Jones et al., 2006; Zheng and Gao, 2000). For controls, explants were electroporated with a vector that expressed either *EGFP* alone or *EGFP* with *Fgf8* in the reverse orientation. Electroporated explants typically contained large clusters of transfected cells in Kolliker's organ, a population of epithelial cells located adjacent to the developing OC (Fig. 5A,B). In control electroporated explants, no changes in PC number, as

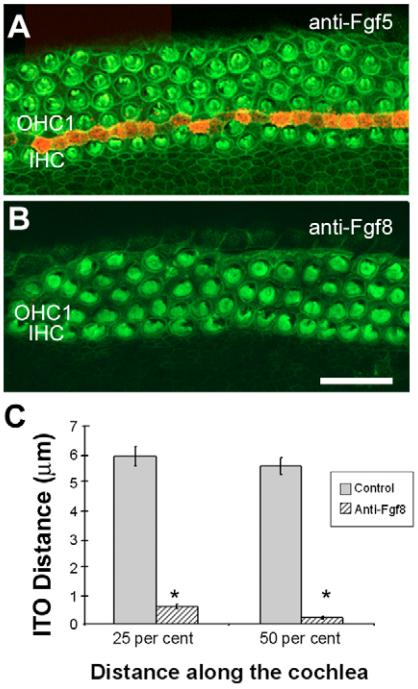

Fig. 4. Inhibition of Fgf8 signaling disrupts pillar cell development. (**A**) A control cochlear explant that was treated with a function-blocking antibody directed against Fgf5. Stereocilia and cell boundaries are labeled with phalloidin (green) and PCs with anti-p75^{ntr} (red). IHCs and first row OHCs are indicated. (**B**) Cochlear explant treated with a function-blocking antibody that binds to Fgf8 (labeling as in B). (**C**) ITO distances for control (anti-Fgf5) and anti-Fgf8-treated explants at basal and midbasal regions of the cochlear duct. *, P<0.001. Scale bar: 20 μm.

determined by expression of p75^{ntr}, were observed in regions of the OC located adjacent to large clusters of transfected cells (Fig. 5A,C). By contrast, there was a marked increase in the number of p75^{ntr}-positive cells, and a decrease in the number of OHCs, in regions of the sensory epithelium located adjacent to large clusters of *Fgf8*-transfected cells (Fig. 5B,D and data not shown). PCs located at a distance from large clusters of *Fgf8*-expressing cells were unaffected, suggesting that Fgf8 has a limited diffusion radius within the cochlear epithelium (Fig. 5B). However, it is also possible that the gradient of Fgf8 is more rapidly decreased because of diffusion into the culture media.

To quantify the effects of overexpression of Fgf8 on p75^{ntr} expression, the relative level of p75^{ntr} (as a measure of the number of PCs) was determined for measured sections of the sensory epithelium located adjacent to regions of Kolliker's organ that were comparably transfected with either the *Fgf8* or control vectors. As a further control, the level of p75^{ntr} in comparable sections of the sensory epithelium was also determined in untransfected explants, or in untransfected regions of transfected explants. Untransfected regions and regions transfected with the control plasmid had similar levels of p75^{ntr} expression, indicating no effect of transfection, or of expression of EGFP, on PC development (Fig. 5E). By contrast, there was a significant increase in the level of expression of p75^{ntr} in regions of the OC located adjacent to *Fgf8*-transfected cells (Fig. 5E). To determine whether a direct correlation exists between the level of *Fgf8* transfection and an increase in p75^{ntr} expression, relative levels of p75^{ntr} were determined for sections of the OC located adjacent to regions of Kolliker's organ with variable levels of transfection. The results indicated a strong positive correlation between increasing levels of *Fgf8*-transfection and the number of p75^{ntr}-positive cells (R^2=0.7405; Fig. 5F), consistent with a dose effect for Fgf8.

Ectopic activation of Fgfr3 increases the expression of pillar cell markers at the expense of outer hair cells

The results presented above are consistent with the hypothesis that an increased level of Fgfr3 activation leads to a greater number of Fgfr3-positive progenitors becoming committed to develop as PCs. Therefore, we sought to fully activate Fgfr3 throughout the developing OC by exposing cochlear explants to Fgf protein. Treatment with Fgf8 protein had no apparent effect on the development of the OC. Although the basis for this is unknown, we were able to obtain a strong effect with Fgf17 protein. To initially confirm that Fgf17 activates Fgfr3 in cochlear explants, explants were exposed to the anti-Fgf8 function-blocking antibody and Fgf17 protein. The presence of Fgf17 was sufficient to rescue PC development in these explants (data not shown).

Treatment with Fgf17 resulted in a conversion of the OHC region of the OC into a band of cells that were positive for p75^{ntr} (Fig. 6A-D). Absence of expression of the hair cell marker myosin VI (Fig. 6E,F) and lack of stereocilia (Fig. 6C,D) indicated that these p75^{ntr}-positive cells were inhibited from developing as OHCs. When a few OHCs were present in Fgf17-treated explants, each was surrounded by a group of p75^{ntr}-negative cells, suggesting that the presence of an OHC was sufficient to cause a local downregulation of p75^{ntr}, even in the presence of Fgf17 (Fig. 6G-I). The effects of Fgf17 treatment appeared to be restricted to the PC/OHC region as myosin VI-positive IHCs were still present in all explants (data not shown). In addition, HeCs located lateral to the OHC domain were also present in Fgf17-treated explants.

Considering that expression of p75^{ntr} is a marker for undifferentiated cells at very early stages of OC development. we wanted to determine whether the large number of p75^{ntr}-positive cells in Fgf17-treated explants represented induction of ectopic PCs, maintenance of undifferentiated cells, or both. β-actin is expressed strongly in PCs and more weakly in OHCs, DCs and HeCs at P0 (see Fig. S1A-F in the supplementary material), but is not expressed in any cell types within the OC prior to E16. Cells which are positive for both p75^{ntr} and β-actin can thus be classified as differentiated PCs. In control explants (established on E13 and maintained for 7 DIV), only the cells located directly adjacent to the IHCs were positive for both p75^{ntr} and β-actin (Fig. 6E). Treatment with Fgf17 resulted in a marked increase in the number of p75^{ntr}-positive cells, with many located throughout the OHC region. However, expression of β-actin was restricted to the cells directly adjacent to the IHCs (Fig. 6F,F′) and to a band of cells located on the lateral edge of the OC, which normally develop as HeCs (Fig. 6F, arrows). The presence of strong p75^{ntr} expression in the absence of β-actin suggests that the effect of activation of Fgfr3 within the OHC region is to inhibit differentiation rather than to induce a PC fate. To confirm this, explants were treated with Fgf17 for 72 hours followed by a 72-hour recovery period. In contrast to the effect of continuous application of Fgf17 (see Fig. S1G in the supplementary material), the patterning of the OC developed normally in explants in which Fgfr3 had been transiently activated. However, OHC development in these explants appeared to be delayed by approximately 72 hours based on the differentiation of OHCs in

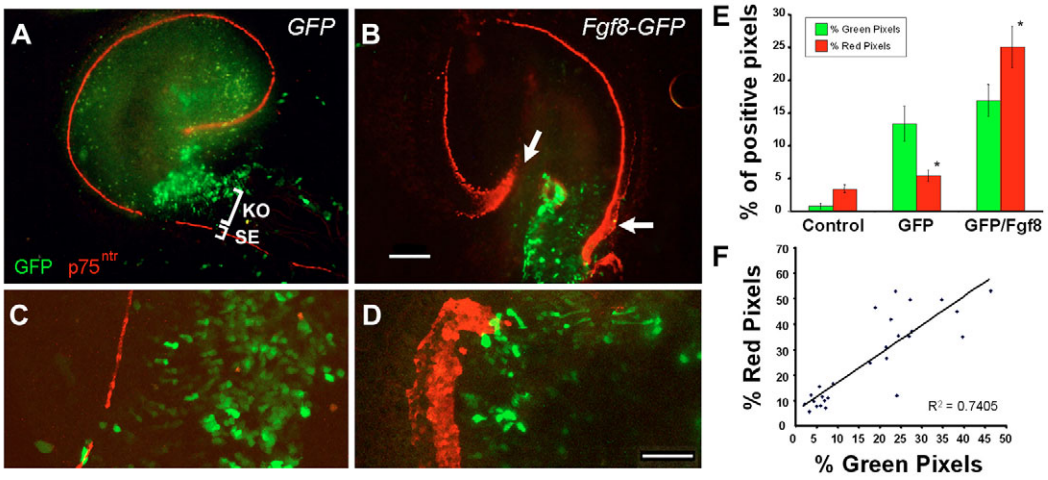

Fig. 5. Overexpression of *Fgf8* induces an increase in p75^{ntr}-positive cells. (**A**) Low-magnification image of a mouse cochlear explant transfected with a control vector expressing GFP (green). The sensory epithelium (SE) is indicated by expression of p75^{ntr} (red) in the PCs. Kolliker's organ (KO) is located medially to the SE. (**B**) Similar view as in A, from an explant transfected with an Fgf8 and GFP-expressing vector (green). p75^{ntr}-positive PCs appear normal except in regions located near a cluster of Fgf8-transfected cells (arrows). (**C**) High-magnification view of a control-transfected cochlea with a large number of transfected cells. (**D**) High-magnification view of an Fgf8-transfected cochlea. Note the increased number of p75^{ntr}-positive cells. (**E**) Quantification of effects of expression of GFP or Fgf8 (green pixels) on p75^{ntr} expression (red pixels); see text for details. Control data represent regions with no electroporation in comparison to regions with high GFP or Fgf8 and GFP electroporation. Error bars indicate s.e.m. *, $P<0.01$. (**F**) A scatter plot of the relationship between the overall level of transfection (% green pixels) and the overall increase in p75^{ntr} expression (% red pixels). Best-fit linear regression line and correlation coefficient (R^2) value are indicated. Scale bars: 100 μm in A,B; 20 μm in C,D.

the second and third rows (see Fig. S1H,I in the supplementary material). These results strongly suggest that activation of Fgfr3 inhibits progenitor cells from developing as hair cells.

To determine whether Fgfr3 activation also promotes PC commitment or differentiation, we examined the effects of treatment with Fgf17 on the development of endogenous PCs. In the presence of Fgf17, PCs developed more rapidly as indicated by larger pillar heads, wider foot plates (Fig. 7, compare A with B, and C with F), and a significant increase in ITO distances versus controls (control, 3.985±0.124 μm; Fgf17-treated, 5.046±0.202 μm; $P<0.0004$).

Treatment with Fgf17 also induced a marked increase in the expression of β-actin (Fig. 6F) and p75^{ntr} (Fig. 7B) in a lateral band of cells that would normally develop as HeCs, suggesting that these cells may assume a PC fate in response to increased activation of Fgfr3. Confocal analysis indicated a marked change in these cells, including increased height, decreased width and maintenance of expression of p75^{ntr} (Fig. 7E,H). Many of these cells developed lumenal projections similar to those of PCs (Fig. 7I-L). Thus, it seems that increased activation of Fgfr3 induces progenitor cells that would normally have developed as HeCs to form as PCs instead.

DISCUSSION

The tunnel of Corti and PCs are unique mammalian structures not found in the elongated cochleae of either birds or reptiles. Although the specific role of the tunnel has not been determined, the shape of the PCs and the position of the tunnel have led to the suggestion that it plays a role in the vibrational isolation of the IHCs. Since a tunnel is only present in the inner ears of mammals, it is generally assumed that the evolution of this structure occurred in response to selective pressures related to increased auditory acuity and perception of high frequencies. The results presented here demonstrate that the development and placement of PCs, and therefore of the tunnel of Corti, are dependent on an inductive interaction between Fgf8, expressed exclusively in IHCs, and Fgfr3, expressed in a domain of progenitor cells located directly adjacent to IHCs. Although Fgfr3 is expressed in progenitors that will develop as OHCs, DCs and HeCs, as well as cells that will develop as PCs, the existing data suggest that the normal range of Fgf8-dependent activation of Fgfr3 is probably limited to the one or two progenitor cells located directly adjacent to the IHC. In addition to the effects of ectopic activation of Fgfr3 by Fgf2 (Mueller et al., 2002), Fgf8 or Fgf17, deletion of the sprouty 2 gene, an Fgf signaling pathway antagonist that is expressed in a similar domain to Fgfr3, results in an extra row of PCs (Shim et al., 2005). These results are consistent with the hypotheses that normal Fgfr3 activation is limited to the cells located directly adjacent to the IHCs and that changes in the spatial activation of Fgfr3, either through increased availability of ligand or through decreased receptor antagonism, results in defects in cellular patterning.

The results presented here coupled with previous findings suggest that Fgfr3 mediates two different aspects of the development of the OC. First, activation of Fgfr3 inhibits the differentiation of cells as OHCs. As discussed, the presence of PCs creates a disruption in the normal alternating cellular mosaic of hair cells and supporting cells. The developmental and evolutionary mechanisms that generate this disruption are unknown, but the data presented here suggest that inhibition of OHC formation through activation of Fgfr3 could represent an import aspect of this regulatory mechanism. This hypothesis is supported by the recent demonstration of an increase in the number of OHCs in Fgfr3 mutants (Hayashi et al., 2007; Puligilla et al., 2007). *Fgfr3* is also expressed in the developing chick basilar papilla (cochlea) but is downregulated in developing hair cells (Bermingham-McDonogh et al., 2001). *Fgfr3* expression is maintained in basilar papilla-supporting cells throughout life, and only becomes downregulated during a regenerative response to hair cell loss (Bermingham-McDonogh et al., 2001). Once hair cells have

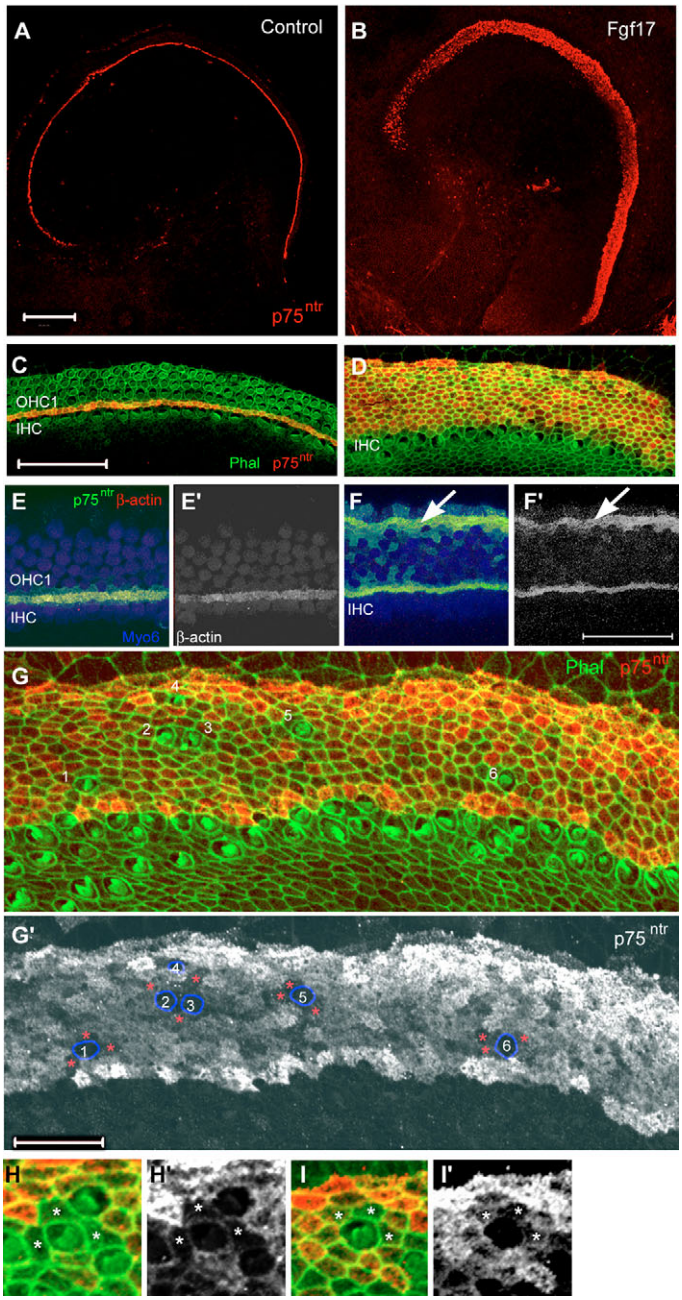

Fig. 6. Fgf17 inhibits development of outer hair cells and Deiters cells. (**A**,**B**) Low-magnification view of $p75^{ntr}$ expression (red) in (A) a control explant and (B) in an explant treated with 300 ng/ml Fgf17 for 5 days. (**C**) High-magnification of a control OC. Cell surfaces and stereocilia are labeled with phalloidin (green), $p75^{ntr}$-positive PCs in red. (**D**) High magnification of an Fgf17-treated explant. IHCs are present, but the OHC region appears undifferentiated and is positive for $p75^{ntr}$ (red). (**E-F′**) Lumenal views of the OC from E14 mouse cochlear explants after 6 DIV. (E) PCs, positive for both $p75^{ntr}$ (green) and β-actin (red), appear as a yellow line between IHCs and OHCs [myosin VI (Myo6) in blue]. (E′) β-actin alone. (F) OHC numbers are reduced and $p75^{ntr}$ expression is increased (green) in the OHC region in Fgf17-treated explants. At the extreme lateral edge, a second band of β-actin expression (red in F, arrow) appears. (F′) β-actin alone. (**G**) An Fgf17-treated explant with few OHCs (numbered). Most cells in the OHC region are positive for $p75^{ntr}$ (red). (**G′**) $p75^{ntr}$ expression alone. OHC positions are indicated with numbered circles. (**H-I′**) High magnification of individual examples of OHCs from Fgf17-treated explants. Stereocilia and cell boundaries are indicated in green, $p75^{ntr}$ in red. Asterisks in G-I′ indicate cells adjacent to OHCs that have downregulated expression of $p75^{ntr}$. Scale bars: 200 μm in A,B; 50 μm in C,D; 20 μm in E-F′; 25 μm in G,G′; 20 μm in H-I′.

been replaced, *Fgfr3* expression returns, suggesting that downregulation of Fgfr3 might be necessary to allow new hair cell formation.

The observation that Fgfr3 expression is maintained in avian supporting cells that retain the ability to develop as hair cells, suggests that expression of Fgfr3 might be an indicator of cells that retain a greater degree of developmental plasticity. Within the adult mammalian cochlea, *Fgfr3* expression is only retained in PCs (Pirvola et al., 1995), suggesting the possibility that these cells might retain a higher degree of cellular plasticity and that ongoing activation of Fgfr3 might be required to maintain PCs in a differentiated state. This hypothesis is supported by the recent demonstration that, in comparison with other cells in the OC, PCs appear to possess a comparatively higher level of plasticity (Izumikawa et al., 2005; Kiernan et al., 2005; White et al., 2006), and may even be able to differentiate into hair cells under some circumstances (White et al., 2006). Based on these results, it seems possible that inhibition of Fgfr3 activation in mature PCs could cause these cells to revert to a less differentiated state. Under some circumstances, it might then be possible to induce these cells to adopt an alternative fate, such as differentiation as a hair cell.

The second role of Fgfr3 appears to be to specify the fate and/or subsequent differentiation of PCs. Deletion of either *Fgfr3* or its endogenous ligand *Fgf8* leads to a disruption in PC differentiation, whereas increased availability of Fgfs enhances the pace of PC differentiation. The induction of ectopic PCs is apparently restricted to a band of cells located on the lateral edge of the OC. The reasons for this restriction are unclear; however, the position of these cells is somewhat similar to the position of the endogenous PCs in that they are located on a border of the OHC domain. Therefore, it seems possible that cells within the OHC domain might be prevented from developing as PCs. This hypothesis is supported by the observation that OHCs were capable of inducing a local decrease in $p75^{ntr}$ even in the presence of Fgf17, suggesting that OHCs or OHC progenitors might exert a local influence that is not compatible with PC development. This type of interaction, along with the limited expression of Fgf8, might play a role in ensuring that PCs only develop between the IHCs and first row OHCs.

The limited expression of Fgf8 in the single row of IHCs, along with the demonstrated roles of Fgfs in the development of PCs and OHCs, suggest that IHCs act as a global organizing center for the development of the OC. Cellular differentiation proceeds in a gradient that begins with the IHCs and moves laterally through the PCs and OHCs. A similar role for Fgf8 has been described during neurogenesis of the chick spinal cord. During development of the neural tube, Fgf8 signals arising from the caudal neural plate act to regulate the timing of neural development within the spinal cord by inhibiting differentiation (Diez del Corral et al., 2002; Diez del Corral et al., 2003), thus maintaining a balance between neuronal and glial cell types. When the Fgf8 signal is removed or inhibited, precocious differentiation of spinal cord neurons is observed (Diez del Corral et al., 2002). Based on the above results, it seems likely

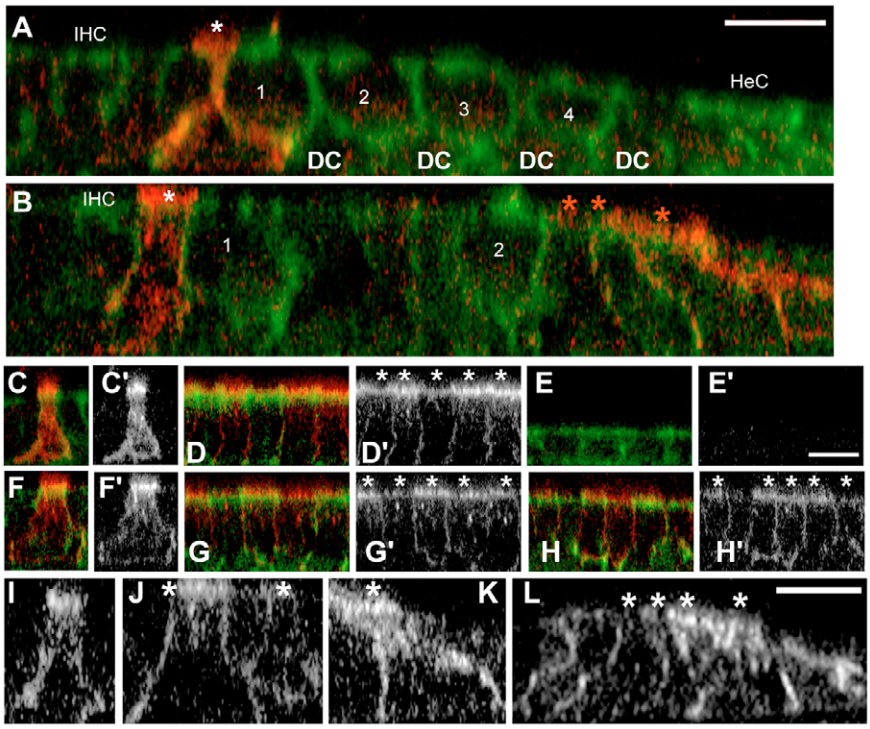

Fig. 7. Fgf17 treatment promotes PC differentiation and induces ectopic PCs. Cross-sections were generated using confocal reconstruction. (**A**) Cross-section through a control explant showing cell boundaries labeled with phalloidin (green), developing PCs (red) and pillar head (asterisk); OHCs are numbered. HeCs located adjacent to OHC4 are short and have weak $p75^{ntr}$ expression. (**B**) An Fgf17-treated explant has a broader pillar head (asterisk), reduced OHC numbers, and three rows of PC-like cells in the HeC position (red asterisks). (**C**,**C′**) High-magnification cross-section of an inner PC (red in C, and shown alone in C′) from a control explant. The pillar head narrows as it approaches the lumenal surface. (**D**,**D′**) Cross-section along the mediolateral plane illustrating the row of inner PCs in a control explant. (**E**,**E′**) Cross-section along the mediolateral plane illustrating the row of HeCs in the same control explant. Note the shortness of the HeCs and lack of $p75^{ntr}$ expression. (**F**) Cross-section through an inner PC from an Fgf17-treated explant. Note the increased width of the pillar head. (**G**,**G′**) Cross-section of PCs from an Fgf17-treated explant, same view as in D. (**H**,**H′**) Cross section of the HeC region from an Fgf17-treated explant. HeCs are taller, are strongly positive for $p75^{ntr}$ and are morphologically similar to PCs (compare with D and G). (**I-L**) Examples of PC (I,J) and HeC (K,L) morphology in control (I) and Fgf17-treated (J-L) explants. All illustrate expression of $p75^{ntr}$. Note the increased thickness of the pillar head in J versus I, and the similarity between endogenous PCs (I,J) and ectopic PCs located in the HeC region (K,L). Asterisks indicate pillar head-like structures. Scale bars: 10 μm.

that Fgf8 signaling may prolong the ability of PCs to switch fates and undergo mitosis. In addition, the expression of multiple sprouty genes within the DCs (Shim et al., 2005) can act to inhibit Fgf8 signaling and, thereby, to also inhibit the ability of DCs to assume a more plastic role within the OC. However, the HeC region never expresses sprouty genes and thus, when exposed to ectopic Fgf8 or Fgf17, can develop as PCs.

Thus, it seems likely that Fgf8 expression by IHCs acts to organize the next step in cellular patterning by inducing the development of PCs and simultaneously preventing the development of hair cells in directly adjacent cells. Following this induction, subsequent signaling interactions must play a role in specifying and patterning the OHCs and associated DCs. Whether these events are regulated through long-range signals generated by IHCs or as a result of shorter-range signals originating in PCs remains to be determined.

We thank Dr Elizabeth Grove for providing the *Fgf8b* expression construct, Chad Woods for technical assistance and Drs Alain Dabdoub and Jennifer Jones for scientific advice. This research was supported by funds from the intramural program at the National Institute on Deafness and other Communication Disorders (M.W.K.) and from the intramural research program of the National Cancer Institute, Center for Cancer Research (M.L.), NIH and by a grant from the United States-Israel Binational Science Foundation 2003335 (M.W.K.).

Supplementary material

Supplementary material for this article is available at http://dev.biologists.org/cgi/content/full/134/16/3021/DC1

References

Bermingham-McDonogh, O., Stone, J. S., Reh, T. A. and Rubel, E. W. (2001). FGFR3 expression during development and regeneration of the chick inner ear sensory epithelia. *Dev. Biol.* **238**, 247-259.

Colvin, J. S., Bohne, B. A., Harding, G. W., McEwen, D. G. and Ornitz, D. M. (1996). Skeletal overgrowth and deafness in mice lacking fibroblast growth factor receptor 3. *Nat. Genet.* **12**, 390-397.

Diez del Corral, R., Breitkreuz, D. N. and Storey, K. G. (2002). Onset of neuronal differentiation is regulated by paraxial mesoderm and requires attenuation of FGF signalling. *Development* **129**, 1681-1691.

Diez del Corral, R., Olivera-Martinez, I., Goriely, A., Gale, E., Maden, M. and Storey, K. (2003). Opposing FGF and retinoid pathways control ventral neural pattern, neuronal differentiation, and segmentation during body axis extension. *Neuron* **40**, 65-79.

Fukuchi-Shimogori, T. and Grove, E. A. (2001). Neocortex patterning by the secreted signaling molecule FGF8. *Science* **294**, 1071-1074.

Fukuchi-Shimogori, T. and Grove, E. A. (2003). Emx2 patterns the neocortex by regulating FGF positional signaling. *Nat. Neurosci.* **6**, 825-831.

Hayashi, T., Cunningham, D. and Bermingham-McDonogh, O. (2007). Loss of Fgfr3 leads to excess hair cell development in the mouse organ of Corti. *Dev. Dyn.* **236**, 525-533.

Hebert, J. M. and McConnell, S. K. (2000). Targeting of cre to the Foxg1 (BF-1) locus mediates loxP recombination in the telencephalon and other developing head structures. *Dev. Biol.* **222**, 296-306.

Izumikawa, M., Minoda, R., Kawamoto, K., Abrashkin, K. A., Swiderski, D. L., Dolan, D. F., Brough, D. E. and Raphael, Y. (2005). Auditory hair cell replacement and hearing improvement by Atoh1 gene therapy in deaf mammals. *Nat. Med.* **11**, 271-276.

Jones, J. M., Montcouquiol, M., Dabdoub, A., Woods, C. and Kelley, M. W. (2006). Inhibitors of differentiation and DNA binding (Ids) regulate Math1 and hair cell formation during the development of the organ of Corti. *J. Neurosci.* **26**, 550-558.

Kiernan, A. E., Cordes, R., Kopan, R., Gossler, A. and Gridley, T. (2005). The Notch ligands DLL1 and JAG2 act synergistically to regulate hair cell development in the mammalian inner ear. *Development* **132**, 4353-4362.

MacArthur, C. A., Lawshe, A., Xu, J., Santos-Ocampo, S., Heikinheimo, M., Chellaiah, A. T. and Ornitz, D. M. (1995). FGF-8 isoforms activate receptor splice forms that are expressed in mesenchymal regions of mouse development. *Development* **121**, 3603-3613.

Meyers, E. N., Lewandoski, M. and Martin, G. R. (1998). An Fgf8 mutant allelic series generated by Cre- and Flp-mediated recombination. *Nat. Genet.* **18**, 136-141.

Mohammadi, M., Olsen, S. K. and Ibrahimi, O. A. (2005). Structural basis for fibroblast growth factor receptor activation. *Cytokine Growth Factor Rev.* **16**, 107-137.

Montcouquiol, M. and Kelley, M. W. (2003). Planar and vertical signals control cellular differentiation and patterning in the mammalian cochlea. *J. Neurosci.* **23**, 9469-9478.
Mueller, K. L., Jacques, B. E. and Kelley, M. W. (2002). Fibroblast growth factor signaling regulates pillar cell development in the organ of corti. *J. Neurosci.* **22**, 9368-9377.
Olsen, S. K., Li, J. Y. H., Bromleigh, C., Eliseenkova, A. V., Ibrahimi, O. A., Lao, Z., Zhang, F., Linhardt, R. J., Joyner, A. L. and Mohammadi, M. (2006). Structural basis by which alternative splicing modulates the organizer activity of FGF8 in the brain. *Genes Dev.* **20**, 185-198.
Ornitz, D. M., Xu, J., Colvin, J. S., McEwen, D. G., MacArthur, C. A., Coulier, F., Gao, G. and Goldfarb, M. (1996). Receptor specificity of the fibroblast growth factor family. *J. Biol. Chem.* **271**, 15292-15297.
Pauley, S., Wright, T. J., Pirvola, U., Ornitz, D., Beisel, K. and Fritzsch, B. (2003). Expression and function of FGF10 in mammalian inner ear development. *Dev. Dyn.* **227**, 203-215.
Peters, K., Ornitz, D., Werner, S. and Williams, L. (1993). Unique expression pattern of the FGF receptor 3 gene during mouse organogenesis. *Dev. Biol.* **155**, 423-430.
Pickles, J. O. (2001). The expression of fibroblast growth factors and their receptors in the embryonic and neonatal mouse inner ear. *Hear. Res.* **155**, 54-62.
Pirvola, U., Cao, Y., Oellig, C., Suoqiang, Z., Pettersson, R. F. and Ylikoski, J. (1995). The site of action of neuronal acidic fibroblast growth factor is the organ of Corti of the rat cochlea. *Proc. Natl. Acad. Sci. USA* **92**, 9269-9273.
Pirvola, U., Ylikoski, J., Trokovic, R., Hebert, J. M., McConnell, S. K. and Partanen, J. (2002). FGFR1 is required for the development of the auditory sensory epithelium. *Neuron* **35**, 671-680.
Puligilla, C., Feng, F., Ishikawa, K., Bertuzzi, S., Dabdoub, A., Griffith, A. J., Fritzsch, B. and Kelley, M. W. (2007). Disruption of fibroblast growth factor receptor 3 signaling results in defects in cellular differentiation, neuronal patterning, and hearing impairment. *Dev. Dyn.* **236**, 1905-1917.
Raphael, Y. and Altschuler, R. A. (2003). Structure and innervation of the cochlea. *Brain Res. Bull.* **60**, 397-422.
Shim, K., Minowada, G., Coling, D. E. and Martin, G. R. (2005). Sprouty2, a mouse deafness gene, regulates cell fate decisions in the auditory sensory epithelium by antagonizing FGF signaling. *Dev. Cell* **8**, 553-564.
Sobin, A. and Anniko, M. (1984). Early development of cochlear hair cell stereociliary surface morphology. *Arch. Otorhinolaryngol.* **241**, 55-64.
Storm, E. E., Rubenstein, J. L. and Martin, G. R. (2003). Dosage of Fgf8 determines whether cell survival is positively or negatively regulated in the developing forebrain. *Proc. Natl. Acad. Sci. USA* **100**, 1757-1762.
White, P. M., Doetzlhofer, A., Lee, Y. S., Groves, A. K. and Segil, N. (2006). Mammalian cochlear supporting cells can divide and trans-differentiate into hair cells. *Nature* **441**, 984-987.
Wu, D. K. and Oh, S.-H. (1996). Sensory organ generation in the chick inner ear. *J. Neurosci.* **16**, 6454-6462.
Zheng, J. L. and Gao, W. Q. (2000). Overexpression of Math1 induces robust production of extra hair cells in postnatal rat inner ears. *Nat. Neurosci.* **3**, 580-586.